Effects of π-Conjugation Attenuation on the Photophysics and Exciton Dynamics of Poly(*p*-phenylenevinylene) Polymers Incorporating 2,2′-Bipyridines

Lin X. Chen,*,† Wighard J. H. Jäger,† Mark P. Niemczyk,† and Michael R. Wasielewski*,†,‡

Chemistry Division, Argonne National Laboratory, Argonne, Illinois 60439-4831, and Department of Chemistry, Northwestern University, Evanston, Illinois 60208-3113

Received: January 21, 1999

The effect of π-conjugation attenuation on the photophysics and exciton dynamics of two conjugated polymers **1** and **2** are examined in solution. The structures of polymers **1** and **2** have 2,2′-bipyridyl-5-vinylene units that alternate with one and three 2,5-bis(*n*-decyloxy)-1,4-phenylenevinylene monomer units, respectively. The photophysics and exciton dynamics of polymers **1** and **2** were compared to those of the homopolymer, poly(2,5-bis(2′-ethylhexyloxy)-1,4-phenylenevinylene) (BEH−PPV). A series of changes in the photophysics of polymers **1** and **2** were found as a result of π-conjugation attenuation. These changes include blue shifts in absorption and emission spectra, spectral diffusion in stimulated emission, enhancement in photoluminescence quantum yields and lifetimes, and increases in photoinduced absorption intensities and lifetimes. These changes are systematically more pronounced in polymer **1** than in polymer **2** and are correlated with π-conjugation attenuation in the polymers due to twisting of the 2,2′-bipyridine groups about the 2,2′ single bond. An exciton dynamics model involving an ensemble of initial exciton states localized on oligomeric segments within the polymer with different conjugation lengths is proposed to describe the observed differences between polymers **1** and **2** and BEH−PPV. When the electronic coupling between these segments is strong, the polymer displays characteristics that are close to those of a one-dimensional semiconductor. However, when these couplings are weakened by groups, such as the 2,2′-bipyridine that attenuate π-conjugation, the polymer displays properties of an ensemble of oligomers.

Introduction

Conjugated polymers, especially poly(*p*-phenylenevinylene) (PPV) based polymers, have been studied extensively from both fundamental photophysical and application aspects because of their potential as materials for light-emitting diodes[1−4] and lasers.[5−7] Recently, several PPV derivatives have been synthesized that explore potential applications in other areas, such as photorefractive materials,[8] metal ion sensing,[9−11] and molecular wires.[12,13] Because photoluminescence of PPV-based polymers is critical in many of these applications, it is important to establish correlations between polymer structural features and fundamental polymer photophysics, such as exciton/polaron generation, migration, and recombination.

Many discussions have focused on whether a π-conjugated polymer should be viewed as a one-dimensional semiconductor or a collection of oligomers with different conjugation lengths.[14] A number of ultrafast optical spectroscopic studies on PPV and MEH−PPV (poly(2-methoxy-5-(2′-ethylhexyloxy)-1,4-phenylenevinylene) revealed the fundamental photophysics of these polymers following initial photoexcitation.[15−19] Three major changes in the optical spectra of PPV derivatives have been observed following photoexcitation: ground-state bleaching, stimulated emission, and photoinduced absorption. There have been numerous debates on the origins of these spectral characteristics. The origin of photoinduced absorption has been assigned to singlet excitons, triplet excitons, polarons, and photooxidized products.[15−28] The origin of stimulated emission has been assigned to a relaxed singlet exciton, a pair of tightly bound polarons, or localized singlet excitons.[15−17,29−33]

In this study, femtosecond transient absorption spectroscopy is used to examine the photophysics of three polymers with different π-conjugation strengths. The homopolymer poly(2,5-bis(2′-ethylhexyloxy)-1,4-phenylene-vinylene) (BEH−PPV) has a backbone structure identical to that of PPV, where its most stable conformation is near-planar.[34] Calculations have predicted that MEH−PPV and BEH−PPV should have nearly planar backbones in their energy-minimized structures. However, the π-conjugation in a planar chain could be perturbed when a group is introduced into the polymer backbone that is capable of achieving a nonplanar conformation. Polymers **1** and **2**[9] are copolymers of BEH−PV (2,5-bis(2′-ethylhexyloxy)-1,4-phenylenevinylene) and bpy (2,2′-bipyridine) with repeating units of $(BEH-PV\text{-}bpy)_n$ and $[(BEH-PV)_3\text{-}bpy]_n$, respectively (Figure 1). Because there is approximately a 20° dihedral angle between two the pyridine planes in its transoid-like conformation and the potential barrier for a rotation along the C−C bond connecting the two pyridine rings is small,[35] nonplanar conformations could exist in polymers **1** and **2**. This deviation from planarity attenuates the π-conjugation in these polymers. As the number of bpy units within the polymer structure increases, π-conjugation in the chain is progressively attenuated, resulting in a series of changes in photophysical properties of polymers **1** and **2**. On the basis of these observations, we will establish correlations between the π-conjugation and photophysical properties of the polymers. To simplify the problem, only dilute solutions of the polymers (10^{-5} M monomer) are studied, where interchain interactions are negligible. In addition, we focus on

* To whom correspondence should be addressed.
† Argonne National Laboratory.
‡ Northwestern University.

10.1021/jp990248e CCC: $18.00
Published on Web 06/03/1999

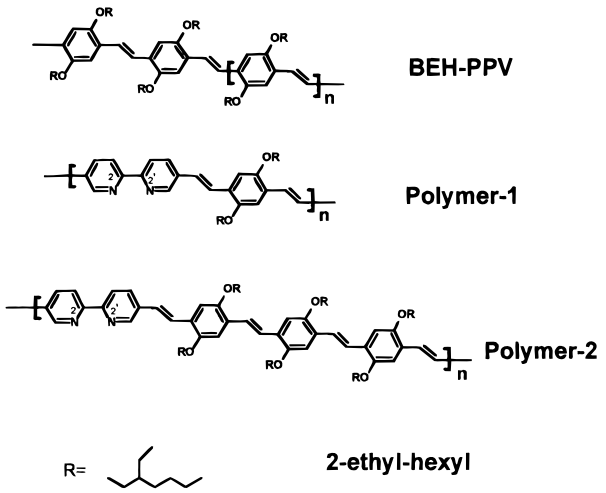

Figure 1. Molecular structures of the polymers. 2,2′ positions in bpy groups are marked.

the first few nanoseconds following photoexcitation so that the dynamics of long-lived species, such as triplet states and distant polarons were excluded. We will first investigate sources of π-conjugation attenuation in polymers **1** and **2**, then systematically study steady-state and transient optical properties of these polymers. Finally, we will explain the observed results in terms of an exciton dynamics model.

Experimental Section

BEH−PPV, polymer **1**, and polymer **2** were synthesized according to the procedures described elsewhere.[9] The molecular weights for BEH−PPV, polymer **1**, and polymer **2** are M_n = 200, 6.4, and 22 kD, respectively. The polymer solids were kept inside a nitrogen box. Toluene (Aldrich) solutions of the polymers were made at concentrations of 1×10^{-5} M or less. Stock solutions were freshly made and checked periodically for photodegradation using UV−visible spectra during the laser experiments. Samples were stirred and changed every hour.

Steady-state optical absorption spectra were measured using a Shimadzu UV−visible spectrophotometer (UV-1601). Corrected fluorescence spectra and relative fluorescence quantum yields were obtained with a Photon Technology International fluorometer. Solutions with 10^{-6} M concentration were used for the fluorescence measurements. All experiments were conducted at room temperature.

Transient absorption measurements were performed with an apparatus based on an amplified Ti:sapphire laser system with an optical parametric amplifier that has been described elsewhere.[36] The excitation pulses were derived from either the second harmonic of the output from the Ti:sapphire amplifier at 417 nm or from an optical parametric amplifier that can generate 470−820 nm light. White-light continuum probe pulses were generated by focusing a few microjoules of the Ti:sapphire amplifier output onto a sapphire disk. The probe beam was split. One beam served as the reference, and the other beam as the probe beam. The probe beam and the 300 nJ pump beam were focused to a 0.3 mm spot size at the sample in a nearly collinear geometry. The optical density of the sample was kept below 0.3, and the path length of the sample cuvette was 2 mm. The lengths of the pump and probe pulses were about 140 fs, and the total instrumental response for the pump−probe experiments was 180 fs. All transient absorption spectra were corrected for temporal chirp in the white-light continuum.

Electronic structure calculations on oligomers of 2,5-dimethoxy-1,4-phenylenevinylene (DMPV) with and without bpy groups

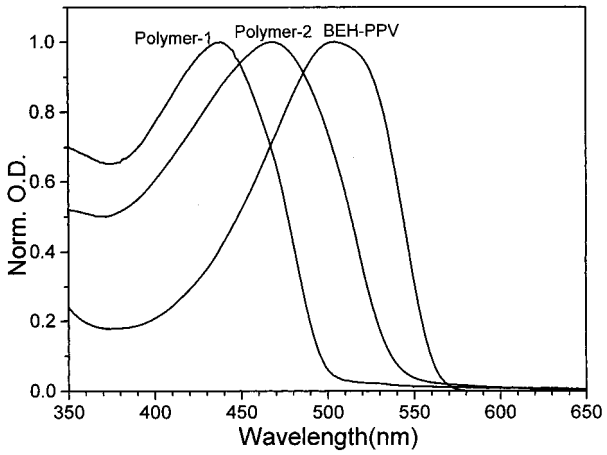

Figure 2. Normalized optical absorption spectra of $\sim 1 \times 10^{-5}$ M polymer solutions in toluene at room temperature.

using the same repeat structures as those of polymers **1** and **2** were performed using the Hyperchem software package (Hypercube Inc.). Using the MM+ force field, each structure was first energy-minimized. Subsequently, single excitation CI calculations using the 10 highest occupied and 10 lowest unoccupied orbitals were conducted using ZINDO/S.[37] The electronic transition energies, as well as the HOMO and LUMO energies, were obtained for each oligomer. The largest oligomer related to polymer **1** for which calculations were performed is $(DMPV-bpy)_4$, while that for polymer **2** is $[(DMPV)_3-bpy]_2$. The same calculation was also performed for $(DMPV)_8$ and $(DMPV-PV)_4$, where PV is an unsubstituted phenylenevinylene fragment.

Results

Observed and Calculated Optical Absorption Spectra. Absorption spectra of BEH−PPV, polymer **1**, and polymer **2** in toluene are presented in Figure 2. Unlike the spectra of phenylenevinylene (PV) oligomers, which display vibronic structure, only a single structureless broad band appears at 504 nm for BEH−PPV in solution. Similar broad absorption bands were also observed at 438 and 468 nm for polymers **1** and **2**, respectively.[9] The blue shifts of the absorption peaks of polymers **1** and **2** relative to that of BEH−PPV in solution are 0.371 and 0.189 eV, respectively. It is well-known that the lowest energy absorption peak red-shifts as the π-conjugation length gets longer.[24] Polymers **1** and **2** are sufficiently long to ensure that the observed absorption shifts are due to their intrinsically shorter conjugation segments rather than their much shorter total chain lengths compared to that of BEH−PPV.[24] Thus, the blue shifts in the absorption peaks indicate that the overall π-conjugation in the BEH−PPV chain has been disturbed because of the insertion of the bpy units in the polymer.

Figure 3 depicts the calculated values of the HOMO−LUMO energy gaps $\Delta E = E_{LUMO} - E_{HOMO}$ as a function of the inverse of the number of bonds, n_B, in the π-conjugated oligomers consisting of DMPV and bpyV (bpy−vinylene) units. The three oligomers $(DMPV)_n$, $(DMPV-bpyV)_n$, and $[(DMPV)_3-bpyV]_n$ correspond to BEH−PPV, polymer **1**, and polymer **2,** respectively. The calculations assumed nearly planar conformations on the basis of energy-minimized structures. A DMPV unit here is used to approximate a BEH−PV monomer. Each of the DMPV and bpy−vinylene units have six and 10 bonds, respectively. The effects of adding a bpyV unit on ΔE are also shown in Figure 3. In the $(DMPV)_n$ case (the dashed lines in all three plots of Figure 3), a linear dependence of ΔE on $1/n_B$

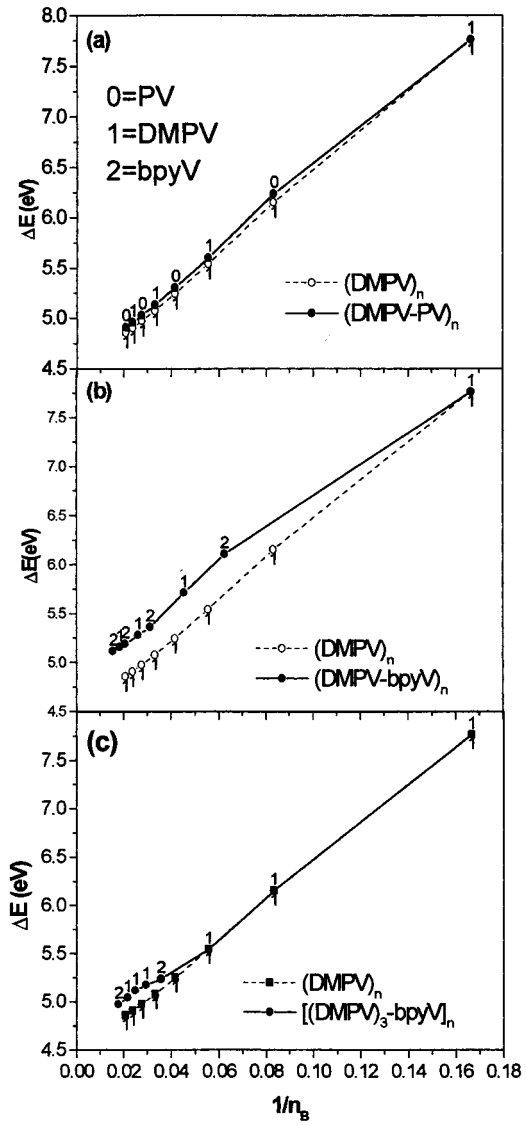

Figure 3. Calculated band gap $\Delta E = E_{LUMO} - E_{HOMO}$ for oligomers with different monomers (0 = PV, 1 = DMPV, 2 = bpy). Relative to the line for the homo-DMPV oligomer, adding PV or bpyV to an existing MPV monomer causes a "kink" in the line that indicates that either PV or bpy monomer attenuates the effect of band gap reduction compared to homo-DMPV case (see text).

is observed. However, when a bpyV unit is added to the π-conjugated system as in (DMPV−bpyV)$_n$ and [(DMPV)$_3$−bpyV]$_n$, the decrease in ΔE caused by extending the π-conjugation length is less than in a homo-DMPV oligomer with an equal number of bonds. In other words, the ΔE value is larger in the hetero-oligomers with DMPV−bpyV than in the DMPV homo-oligomers of equal length. This effect creates a "kink" in the ΔE vs $1/n_B$ plot that makes the curve deviate from that of the DMPV oligomers.

Calculated results for the lowest energy optical transition energy E_{min} are shown in Figure 4. The number of bonds required to saturate E_{min} values are similar for all three polymers. However, adding a bpy unit to a π-conjugated DMPV unit reduces E_{min} less than adding an additional DMPV unit. Similarly, adding a bpy unit to the (DMPV)$_3$, mimicking the situation in polymer **2**, also causes the same effect as in polymer **1** but to a lesser extent. Both planar *syn*- and *anti*-2,2′-bpy conformations were used in the calculations, and the differences in the results were shown to be negligible. The results presented here assumed all *syn*-2,2′-bpy segments in the polymer chains. The calculated results in Figures 3 and 4 are strong evidence of π-conjugation attenuation caused solely by weakened electronic interactions between adjacent units with different electronic structures.

We then examined the π-conjugation attenuation due to nonplanar conformations. The ΔE difference for a (DMPV)$_3$−bpy−(DMPV)$_3$ oligomer as a function of the N−C−C−N dihedral angle φ within bpy for $\varphi = 0°$ and 90° was calculated. These values of the dihedral angle correspond to planar and orthogonal conformations between the two halves of the oligomers, respectively. The ΔE difference is 0.133 eV, implying that a 15 nm blue shift may be observed due to the conformational change from planar to orthogonal on the basis of an approximate linear relationship between ΔE and E_{min} in the DMPV series. Not surprisingly, the π-conjugation between the two halves of the oligomer is minimized in the orthogonal conformation.

Photoluminescence Spectra and Relative Photoluminescence Quantum Yields. One likely cause of the breadth of the low-energy absorption bands of the polymers in solution is the existence of various oligomeric segments along the polymer chain that have different π-conjugation lengths. The segments with longer π-conjugation lengths should absorb on the red side of the absorption bands. If this assumption is true, knowing the efficiency of energy transfer among these segments is important. Selective excitation at different wavelengths within an absorption band was carried out to address this issue.[38] If a segment with a particular π-conjugation length is selectively excited and if the exciton residing on it does not interact strongly with other parts of the polymer chain, a unique emission spectrum should be observed for a particular excitation wavelength λ_{ex}.[38] On the other hand, if there are strong interactions between different parts of the chain with fast exciton relaxation along the polymer chain to the lowest energy emitting state, the emission spectra should be λ_{ex}-independent.

Figure 5 displays the steady-state emission spectra of the polymers with different λ_{ex}, along with their respective absorption spectra. The emission spectra of BEH−PPV and polymer **2** show almost no λ_{ex} dependence, whereas the emission spectra of polymer **1** show a slight λ_{ex} dependence at the lower energy vibronic peak around 540 nm. These results indicate that the emitting species from each polymer is largely independent of the initial excitonic species at room temperature in solution, at least on a relatively long time scale.

The photoluminescence quantum yields of polymers **1** and **2** relative to that of BEH−PPV were obtained from the corrected fluorescence spectra of the polymers in Figure 6. The relative fluorescence quantum yields for polymers **1** and **2** are 1.9 and 1.5 times that of BEH−PPV, which is 0.3. The 0−0 transitions in the photoluminescence spectra occur at 17 900, 18 500, and 20 133 cm^{-1} for BEH−PPV, polymer **2**, and polymer **1**, respectively. This quantum yield enhancement is important from the point of view of device applications of these polymers.

Excitation Wavelength Dependence of Stimulated Emission and Photoinduced Absorption. Although little excitation wavelength, λ_{ex} dependence was observed in the steady-state photoluminescence spectra of the polymers, some variations in stimulated emission spectral regions were detected on a femtosecond to picosecond time scale when λ_{ex} was varied. The initial transient spectra at 1−2 ps after the excitation pulse for the three polymers with different λ_{ex} are displayed in Figure 7. For BEH−PPV, laser pulses at 417, 512, and 555 nm were used, for polymer **2**, 417, 512, and 536 nm, and for polymer **1**, only 417 nm. For BEH−PPV, little λ_{ex} dependence of the transient

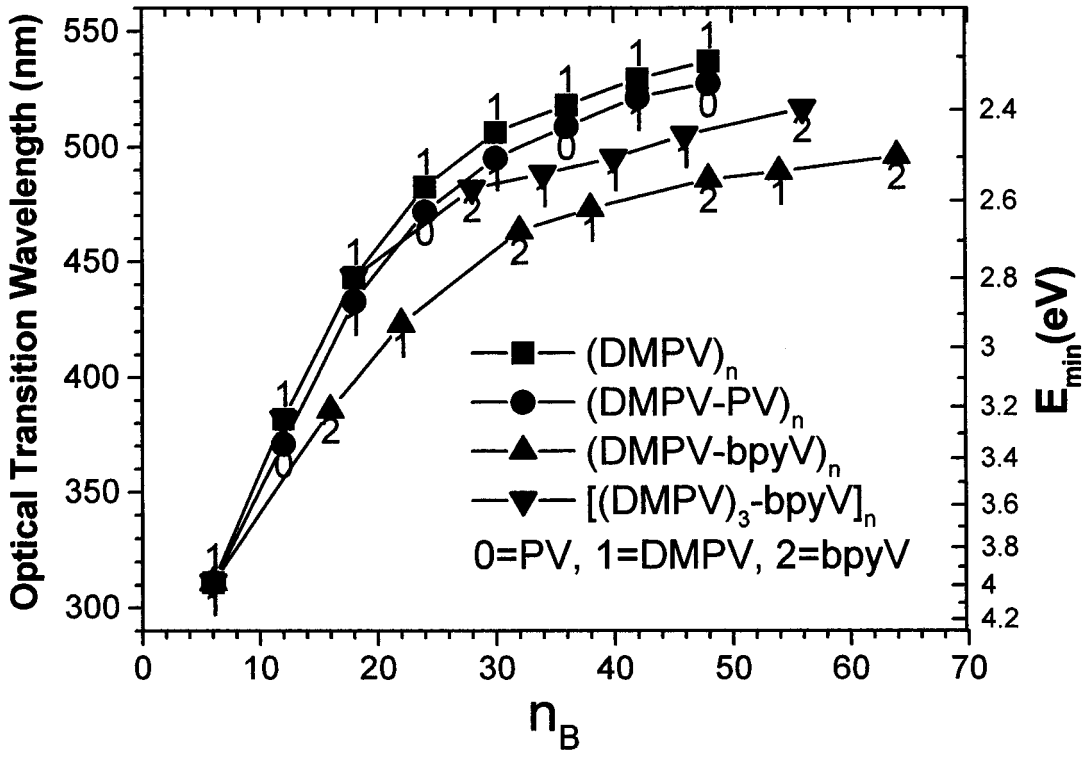

Figure 4. Calculated E_{min} and corresponding optical transition wavelength in various oligomers as in Figure 3.

spectra was observed in both the stimulated emission (560−680 nm) and the photoinduced absorption (>700 nm) regions (Figure 7a). The transient spectra with different λ_{ex} in the stimulated emission region agree well with the fluorescence spectrum. The stimulated emission and the fluorescence spectra are very similar in the vibronic band around 605 nm with different λ_{ex}. The 0−0 transition occurs where the spectral regions of the stimulated emission and ground-state bleaching (<580 nm) overlap and thus is not used to compare the spectra. The λ_{ex} invariance in stimulated emission spectra at 1−2 ps after the photoexcitation for BEH−PPV agrees well with previous results reported for PPV and MEH−PPV in solution,[15,17,29,33] where primary exciton relaxation was completed within 1 ps. This indicates that although selected oligomeric segments along the polymer chain with different π-conjugation lengths were preferentially excited, the initial exciton rapidly decays to the same Stokes shifted state from which the photoluminescence originates. The total integrated intensity of photoinduced absorption (>700 nm) for BEH−PPV shows a slight increase as the excitation photon energy increases.

Polymer **2** exhibits λ_{ex} dependence in its transient spectra in both the stimulated emission (530−670 nm) and photoinduced absorption (>620 nm) spectral regions. Compared to BEH−PPV, the integrated intensities of photoinduced absorption for polymer **2** increase more significantly as the excitation photon energy increases, and the overall integrated intensities of the photoinduced absorption compared to the stimulated emission intensities are greater than that observed for BEH−PPV. When the excitation photon energies are much higher than the 0−0 transition energy, the initial stimulated emission for polymer **2** deviates from its photoluminescence spectra. This deviation diminishes as the excitation photon energy decreases. Excitation with 536 nm light at the red edge of the absorption peak produced the initial stimulated emission that agrees with the photoluminescence spectrum.

An even greater deviation in the stimulated emission region (480−650 nm) was observed for polymer **1** than for polymer **2** using 417 nm excitation. Stimulated emission observed at early times at 490−600 nm even failed to reproduce the vibronic peak at about 530 nm in polymer **1**. This vibronic structure observed in the stimulated emssion spectrum of polymer **1** evolves to that observed in its steady-state fluorescence spectrum ~100 ps following excitation. The integrated intensity of the photoinduced absorption observed in polymer **1** is even higher than that for polymer **2** relative to its stimulated emission peak. Thus, the λ_{ex} dependence of stimulated emission and integrated intensities of photoinduced absorption increase as the linear density of the π-conjugation attenuator bpy increases within the polymer chains.

Spectral Diffusion of Stimulated Emission. The photoluminescence spectra of polymers **1** and **2** show little dependence on λ_{ex}, whereas the initial stimulated emission spectra at early times following excitation are λ_{ex}-dependent and deviate from the photoluminescence spectra when the excitation photon energies are well above the 0−0 transition. Therefore, the initial stimulated emission spectra in polymers **1** and **2** are expected to evolve with time, via spectral diffusion, into the spectra that resemble the photoluminescence spectra. The dynamics of the spectral diffusion provide information on intrachain electronic interactions in the polymers.

Figure 8 presents the time evolution of the red side of the stimulated emission for the polymers with 417 nm excitation, which is well above the energies of the 0−0 transitions. BEH−PPV shows virtually no change in spectral shape 2 ps following excitation. However, both polymers **1** and **2** show continuous red shifts of their respective spectra during the first 50−100 ps after the excitation. Polymer **2** finishes the spectral shift within 50 ps, while polymer **1** finishes 100 ps following the excitation. During the time period 2−50 ps following excitation, the red edge of the stimulated emission for polymer **2** has shifted about 18 nm to the red, resulting in a stimulated emission spectrum that resembles the photoluminescence spectrum. The stimulated emission spectral diffusion is more obvious in polymer **1** and proceeds in two stages. Between 1 and 3 ps the red edge shifts

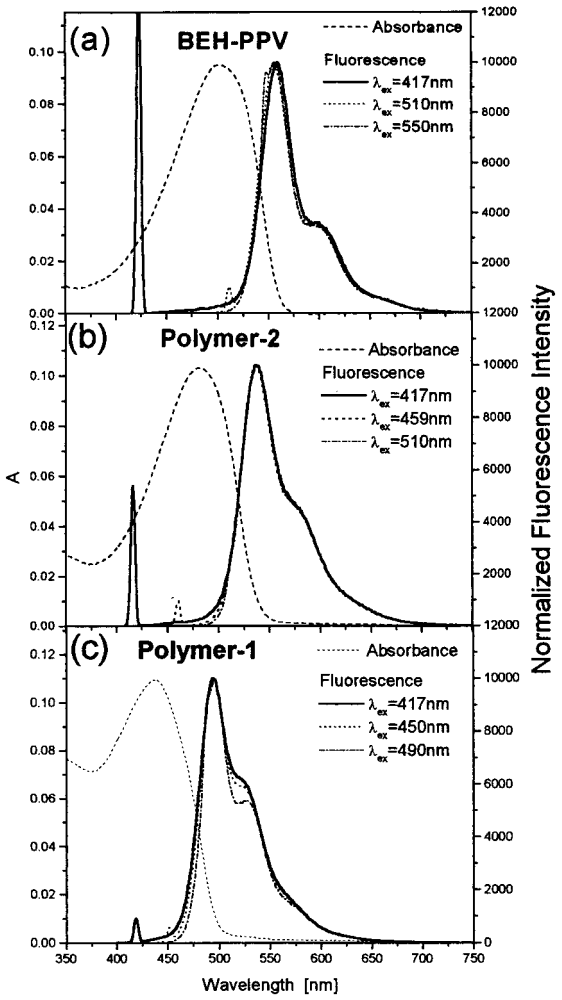

Figure 5. Steady-state fluorescence spectra (uncorrected for wavelength dependence) of polymers in toluene with different excitation wavelengths.

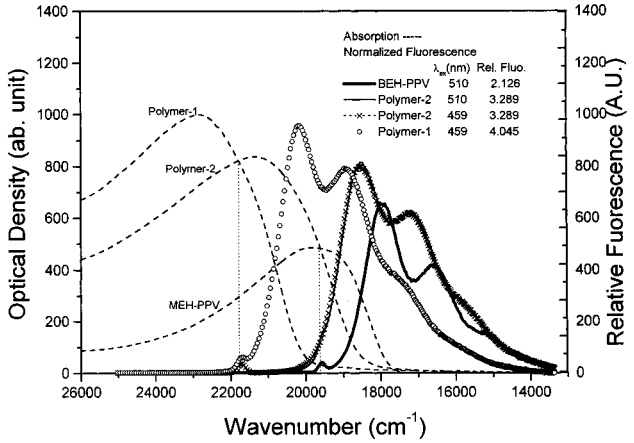

Figure 6. Relative steady-state fluorescence spectra of polymers in toluene normalized by the same optical densities. The results were obtained by normalizing the fluorescence intensities of solutions of polymers **1** and **2** to their optical densities (OD) at 459 nm, where they were excited, and repeating the same process again for polymer **2** and BEH−PPV at 510 nm. The areas under the fluorescence spectra represent the relative fluorescence quantum yields. The dashed curves are the absorption spectra of the polymers, and the dashed vertical lines mark the excitation photon energies at 19 607 cm^{-1} (510 nm) and 21 786 cm^{-1} (459 nm).

by about 10 nm, remains the same between 5 and 10 ps, then continues to shift another 12 nm to the red between 5 and 100

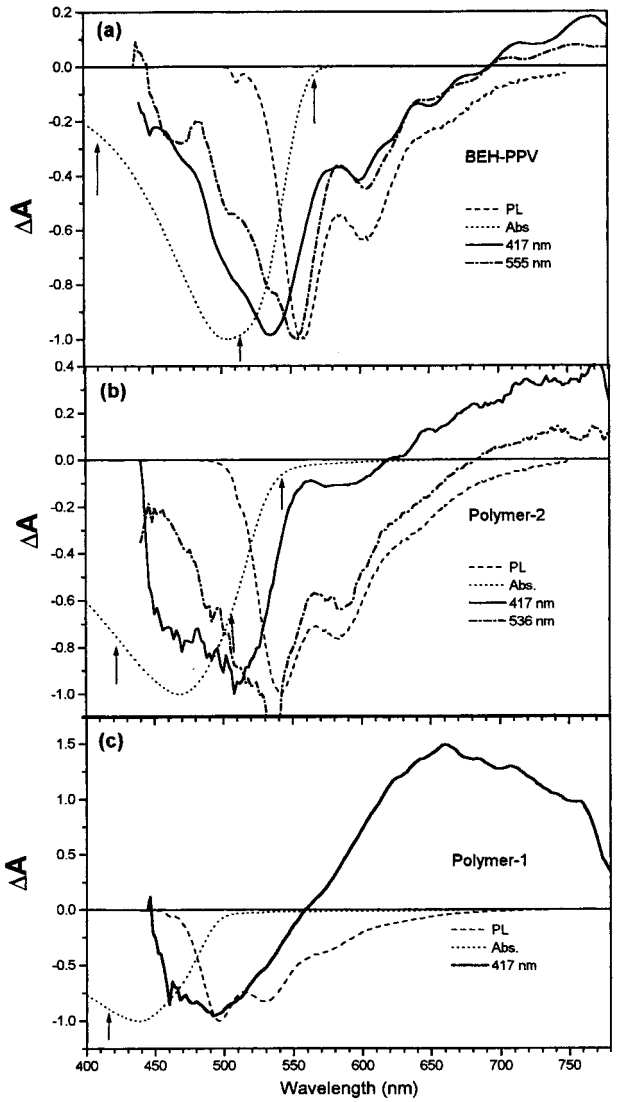

Figure 7. Transient absorption spectra of (a) BEH−PPV, (b) polymer **2**, and (c) polymer **1** in toluene with different λ_{ex} at 2 ps along with absorption spectra (dotted lines) and photoluminescence spectra (dashed lines). The upward arrows indicate the excitation wavelengths and their locations in the absorption bands. The transient absorption spectra at 512 nm for BEH−PPV and polymer **2** are not shown in order to simplify the figures.

ps, resulting in the lower energy vibronic feature of the photoluminescence spectrum at about 530 nm. This two-stage spectral evolution was also observed in the photoinduced absorption spectra, where a broad band arose from 1 to 3 ps, then decayed between 5 and 10 ps, and subsequently evolved into a double-peaked broad band at about 100 ps after the excitation. The deviation in the initial stimulated emission spectra in polymers **1** and **2** from their photoluminescence spectra and the continuous red shifts of the edge of the stimulated emission following the excitation indicate that the initial excited states have higher energies than the final relaxed photoluminescence state. The longer time required to finish the spectral red shifts for polymers **1** than for polymer **2** suggests that the relaxation time from the initial excited states to the final emitting states increases as the polymer π-conjugation is attenuated by more bpy groups in the polymer chains.

Photoinduced Absorption Decay Kinetics. Although the origin of photoinduced absorption in PPV polymers remains an unsettled issue, it is certain that the photoinduced absorption decays monitored between 720 and 775 nm shown in Figure 9

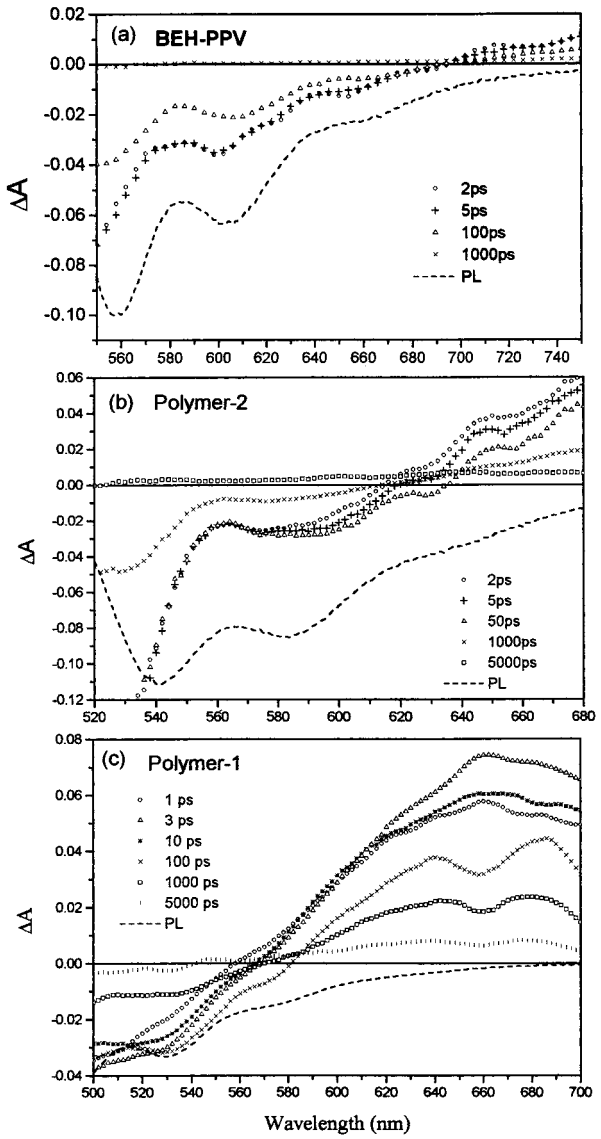

Figure 8. Time evolution of the stimulated emission for (a) BEH−PPV, (b) polymer **2**, and (c) polymer **1** in toluene at room temperature with 417 nm excitation.

reflect the dynamics of both radiative and nonradiative processes of the polymer excited states. Because of the uncertainty in the identities of the states involved, it is difficult to quantitatively describe the kinetics in the photoinduced absorption region. In this study, decays of photoinduced absorption are fit to two or three exponential components as listed in Table 1. Obviously, fitting with multiple exponential kinetics assumes that all the processes are unimolecular, which is clearly not true for exciton−exciton annihilation and spatially indirect exciton formation and recombination. However, such processes are minimized in dilute polymer solutions with relatively low excitation photon fluxes. Because of spectral overlaps for a number of possible absorbing species of the excited states, solving the kinetics of each individual component is always a challenge. In this section, we concentrate on the effect of inserted bpy groups on the photoinduced absorption kinetics of polymers **1** and **2** compared to that of BEH−PPV. A parallel analysis is conducted in the kinetics data for all the polymers.

With multiexponential fits, the dominant component in the photoinduced absorption decay of each polymer is the one with the longest decay time constant, which increases with the number of bpy groups inserted in the polymer chain. There is

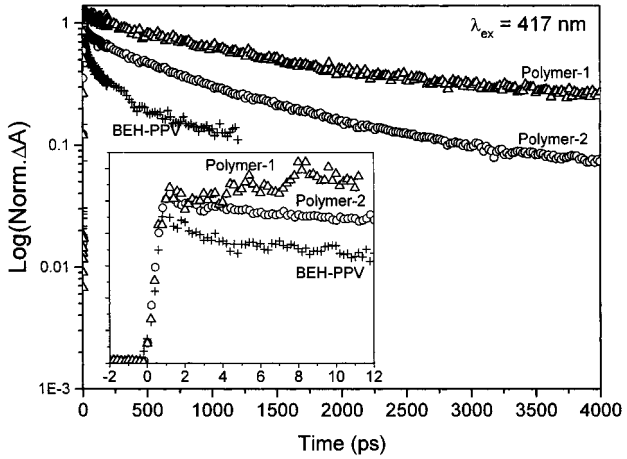

Figure 9. Photoinduced absorption decays of the polymers in toluene with excitation at 417 nm. The inset expands the decays at early time.

a 2-fold to 4-fold increase in the decay time constant from 220 ps for BEH−PPV to 470−1000 ps for polymer **2** (varies with λ_{ex}) and to 1300 ps for polymer **1** (λ_{ex}= 417 nm). Because our femtosecond transient spectroscopic measurements are limited to a time window of a few nanoseconds, the decay components with time constants substantially longer are not included, such as those that describe triplet exciton decay. Therefore, the main components for the polymers listed in Table 1 with time constants from 200 to 1300 ps reflect the lifetimes of singlet excitonic species.

Table 1 shows the λ_{ex} dependence of the excited-state kinetics. A noticeable difference in the kinetics is the effect of λ_{ex} on the time constant τ_1 of the major component. The time constant τ_1 varies by 5% for BEH−PPV from 218 to 229 ps as λ_{ex} varies from 417 to 555 nm, whereas τ_1 varies over 100% for polymer **2** from 468 to 1017 ps as λ_{ex} varies from 417 to 536 nm. As the excitation energy increases above the 0−0 transition in polymer **2**, the apparent lifetime of the exciton state becomes longer due to relaxation of the initial exciton to the emitting exciton state. The time required for this process is shorter, when the emitting state is produced directly as is the case for 536 nm excitation at the red edge of the polymer **2** absorption band. Therefore, the excited-state dynamics are slowed by the presence of bpy in polymer **2**. With this trend in mind, the photoinduced absorption changes for polymer **1** having a 16 ps rise time and a relatively slow decay time of 1300 ps is not unexpected. Changes in spectral shape within the first 100 ps after excitation provide evidence for exciton diffusion in search of the emissive state (Figure 8).

The inset of Figure 9 shows the time evolution of the photoinduced absorption during the first several picoseconds after excitation at 417 nm. By use of a multiexponential fit, BEH−PPV has a fast decay component with a time constant of ∼1 ps, whereas in polymer **2** this decay component increases to 5 ps, while polymer **1** has a rise component of 16 ps as well as a decay component 26 ps. The lack of λ_{ex} dependence observed in BEH−PPV and a less than 1 ps decay component in the exciton decay kinetics suggest that the initial exciton relaxation occurs on a subpicosecond time scale. In contrast, the 5 ps decay component observed in polymer **2** could arise from exciton migration that is significantly slowed because of attenuated π-conjugation by the bpy groups. More interestingly, the photoinduced absorption for polymer **1** rises and then decays. The additional bpy groups in polymer **1** not only slow exciton migration but in addition retard exciton formation, which will be discussed in detail below.

TABLE 1: Photoinduced Absorption Kinetics of Polymers in Toluene at 293 K

polymer	A_1 (%)	τ_1 (ps)	A_2 (%)	τ_2 (ps)	A_3 (%)	τ_3 (ps)
BEH−PPV (λ_{ex} = 417 nm)	56	218 ± 14	28	18 ± 4	16	1 ± 0.1
BEH−PPV (λ_{ex} = 512 nm)	42	222 ± 9	31	23 ± 2	27	1 ± 0.2
BEH−PPV (λ_{ex} = 555 nm)	68	229 ± 7	18	18 ± 3	14	0.7 ± 0.2
polymer **2** (λ_{ex} = 417 nm)	67	1017 ± 34	17	106 ± 15	16	5 ± 0.6
polymer **2** (λ_{ex} = 512 nm)	70	802 ± 9	20	58 ± 5	10	5 ± 0.8
polymer **2** (λ_{ex} = 536 nm)	84	468 ± 32	16	46 ± 14		
polymer **1** (λ_{ex} = 417 nm)	59	1303 ± 28	41	26 ± 4		16 ± 3[a]

[a] Rise time.

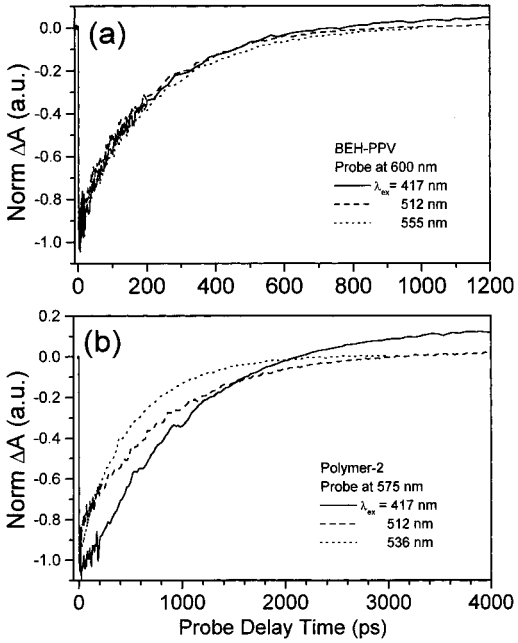

Figure 10. Stimulated emission decays of (a) BEH−PPV and (b) polymer **2** in toluene with different excitation wavelengths.

Stimulated Emission Decay Kinetics. The photoluminescence decay kinetics for the polymers were monitored by stimulated emission at the first vibronic peak of the photoluminescence spectrum, where minimum interference from the bleaching of the ground-state and the excited-state absorption bands is anticipated. Figure 10 shows normalized stimulated emission decays for BEH−PPV monitored at 600 nm and for polymer **2** at 575 nm, with different λ_{ex}. Similar to the photoinduced absorption decay, the stimulated emission decay kinetics of BEH−PPV is nearly λ_{ex}-independent (see Table 2). The λ_{ex} dependence of the time constant τ_1 for the major component of polymer **2** agrees with what was observed in its photoinduced absorption decays, suggesting a correlation between the two processes. The influence of π-conjugation on exciton relaxation described for the photoinduced absorption results can be observed in the kinetics of stimulated emission as well. Compared to the photoinduced absorption kinetics, where the fraction of the major component was 46−84%, the relative fraction of the major component in the stimulated emission kinetics is much higher at 80−93%. The reason for this increase is due to the fact that nonradiative species will not have an optical absorption in this region. Since the photoluminescence decay is a well-known one-body process, the time constants obtained here will be valid values for the lifetimes of the emitting exciton states. It is also possible that the minor component here is due to excited-state absorption that overlaps the stimulated emission region.

Correlations of the Stimulated Emission, Photoinduced Absorption, and the Ground-State Bleaching Kinetics. One way to identify the origins of the species causing the transient absorption is to look for correlations in the kinetics for spectral changes in different regions. Figure 11 demonstrates such kinetic correlations in BEH−PPV and in polymer **2** from plots of normalized absorption changes for the ground-state bleaching, stimulated emission, and photoinduced absorption as a function of the probe delay time. For polymer **2**, the three kinetic traces overlap at times within 1 ns and deviate from each other in the longer time. In contrast, the three kinetic traces are poorly overlapped for BEH−PPV. The agreement between different kinetics traces in polymer **2** indicates that the same species are responsible for the photoinduced absorption emission and that the nonradiative processes are negligible within 1 ns. However, the deviation between the three kinetic traces at longer time suggests that nonradiative species may be generated later, such as triplet states. The poor correlation among the three kinetics traces for BEH−PPV indicates that the different species are responsible for the transient absorption changes in different regions. The initial fast decay of the ground-state bleaching (the inset of Figure 11a) likely involves nonradiative species that do not absorb or emit light at the observed wavelengths because this component is absent in both stimulated emission and photoinduced absorption. However, the fast rise component in stimulated emission and the fast decay component correlate well with each other during the first few picoseconds after photoexcitation. The discrepancy occurs later, most likely through formation of nonradiative species.

Discussion

Sources of π-Conjugation Attenuation by bpy Groups in Polymers 1 and 2. Insertion of bpy units in an otherwise well-conjugated polymer chain brings about structural changes that diminish π-conjugation in the polymer chain. The attenuation of π-conjugation by a bpy unit is due primarily to two phenomena. First, the electronic coupling between two neighboring monomers is reduced because the electronic structure of bpy differs significantly from that of the BEH−PV monomer. Second, a rotation about the C−C bond connecting the two pyridyl rings of bpy results in nonplanar conformations between two adjacent well-conjugated segments of the polymer, also causing reduced π-orbital overlap.

The first phenomenon can be examined by comparing the π-electron density overlap between two adjacent BEH−PV monomers with that between adjacent BEH−PV and bpy groups assuming all-planar conformation. When two identical groups are brought together, the electron density overlaps among π orbitals are most favorable because the symmetry of the orbitals and the energy levels are the same. In this case, the electronic interactions are strong and there is little energy barrier between the two groups preventing the π-electron delocalization. When two adjacent groups have different symmetries and orbitals energies, the π-electron density overlap will be reduced. If such differences are large, there will be no significant π-electron

TABLE 2: Photoluminescence Decay Kinetics of Polymers in Toluene at 293 K

polymer	A_1 (%)	τ_1 (ps)	A_2 (%)	τ_2 (ps)	τ_3 (ps)[a]
BEH−PPV					
(λ_{ex} = 417 nm, λ_{probe} = 600 nm)	80	256 ± 10	20	45 ± 8	0.4 ± 0.08
(λ_{ex} = 512 nm, λ_{probe} = 600 nm)	89	220 ± 11	11	27 ± 10	0.6 ± 0.08
(λ_{ex} = 555 nm, λ_{probe} = 600 nm)	91	219 ± 4	9	8 ± 2	1 ± 0.6
polymer **2**					
(λ_{ex} = 417 nm, λ_{probe} = 575 nm)	86	1031 ± 25	14	14 ± 2[a]	0.5 ± 0.1
(λ_{ex} = 512 nm, λ_{probe} = 575 nm)	85	864 ± 11	15	14 ± 2	0.6 ± 0.8
(λ_{ex} = 536 nm, λ_{probe} = 575 nm)	93	501 ± 3	7	17 ± 3	0.7 ± 0.2

[a] Rise time.

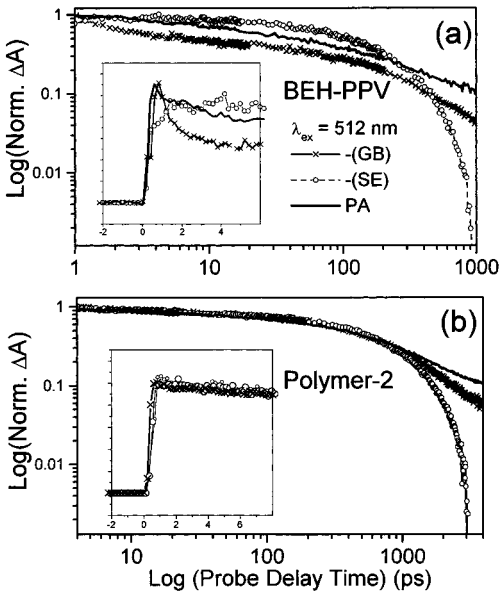

Figure 11. Normalized kinetics traces of the ground-state recovery, stimulated emission, and photoinduced absorption for (a) BEH−PPV and (b) polymer **2** in toluene solution at room temperature, excited by 512 nm light.

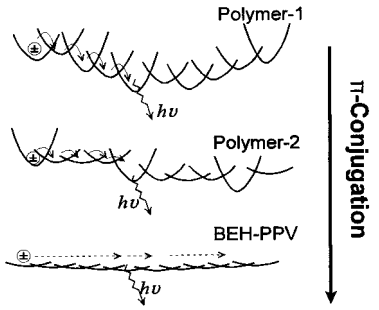

Figure 12. Potential barriers across the polymer chains. The barrier height is higher when a bpy group is inserted because of the nonplanar conformation and weakened electronic interactions between bpy and BEH−PV groups. In segments where all groups are BEH−PV, the barrier heights are depicted lower because of stronger π-conjugation.

overlap between the groups, and the electrons will be localized within each monomer segment.

As an immediate result of π-orbital interactions between two identical adjacent groups, the HOMO energy increases while the LUMO energy decreases, which leads to reduction of the energy gap, ΔE. However, this reduction in ΔE is smaller if the two interacting groups have different electronic structures. Figure 3 shows this by comparing ΔE vs $1/n_B$ plots of the three hetero-oligomers with a homo-DMPV oligomer. All three hetero-oligomers, $(DMPV-PV)_n$, $(DMPV-bpyV)_n$, and $[(DMPV)_3-bpyV]_n$, result in higher ΔE than a homo-DMPV oligomer with the same number of π-conjugated bonds. Similarly, the lowest energy transition, E_{min}, corresponding to the optical absorption band, is more red-shifted in homo-oligomers than hetero-oligomers with the same number of π-conjugated bonds (Figure 4) as oligomers get longer. As a result of the π-conjugation reduction by the electronic structural differences between different groups, a potential barrier for electron or hole delocalization across the boundary of the groups is formed along the polymer chain. The weaker the interactions between the groups, the higher the barrier is for the electron delocalization. Depending on these potential barrier heights, conjugated polymers manifest the characteristics of either one-dimensional semiconductors or ensembles of molecular chromophores, as well as a spectrum of intermediate characteristics.

The second reason that the bpy groups in polymers **1** and **2** weaken π-conjugation is the nonplanar conformation along the polymer chain caused by a rotation along the C−C bond joining the two pyridines. In a bpy group, the potential energy barrier between a planar conformation and the orthogonal conformation is only about 0.025 eV[35] compared to 3.467 eV for rotating a C=C double bond in stilbene.[39] This comparison implies that bpy groups in polymers **1** and **2** act as swivel points to disconnect two adjacent π-conjugated sections in the polymer chain. Similar effects have been investigated through a series of calculations on poly(*p*-pyridylvinylene−phenylenevinylyene)s where the blue shift of the polymers could be modeled by the out-of-plane torsional movements of the pyridyl rings.[40] Naturally, these torsional movements that lead to nonplanar conformations also contribute to the potential barriers that prevent π-electron delocalization along the polymer chain. In addition, the torsional angles are changing with time in solution, and so are the barrier heights, resulting in a dynamic change in segment conjugation lengths along the polymer chain. Therefore, the blue shifts in the absorption bands for polymers **1** and **2** are due to both the electronic structure differences and nonplanar conformations. Their influence on the energy gap and on the lowest absorption band measured in the experiments is comparable and should be considered.

Exciton Dynamics Model for Polymers with π-Conjugation Attenuation. On the basis of the discussion above, in the order of BEH−PPV, polymer **2**, and polymer **1**, the π-conjugation of the polymer chain is increasingly attenuated, corresponding to an increase of potential barrier heights for electron delocalization as shown in Figure 12. Consequently, changes in the photophysics of the polymers have been observed as presented in Results. To establish a correlation between the π-conjugation along the polymer chain and its photophysics, an exciton dynamics model for isolated polymer chains at early times following photoexcitation is proposed.

A three-state exciton dynamics model depicted in Figure 13 involves the ground state, the initial exciton state, and the relaxed emissive exciton state. The initial exciton state is a localized exciton created via direct photoexcitation, which can proceed through an energy transfer cascade either to a relaxed emissive

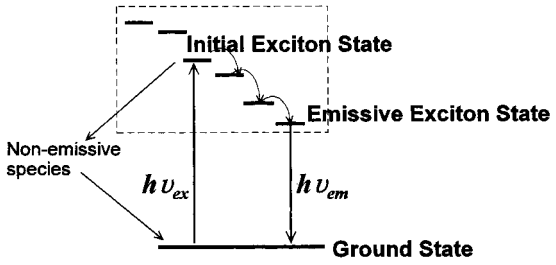

Figure 13. Three-state exciton dynamics model.

exciton state or to a nonemissive species, which returns to the ground state via radiative and nonradiative processes, respectively. Excitation with higher energy photons will preferentially create initial excitons residing on segments with shorter conjugation lengths, whereas lower energy photons will preferentially excite the segments with longer conjugation lengths. The higher the initial exciton energy, the longer will be its relaxation to the final emissive exciton state. This model is used in conjunction with the potential barrier diagrams in Figure 12 to explain the changes in polymer photophysics as the π-conjugation along the polymer backbone is progressively attenuated.

On the basis of previous studies, the photoluminescence of photoexcited PPV polymers originates from localized singlet exciton states.[15,20,21] An emissive singlet exciton state with π-electron delocalization over six units has been suggested on the basis of the resemblance of the photoluminescence to that of the oligomers.[41] Because of the λ_{ex} invariance of the lifetimes for the photoinduced absorption and stimulated emission of MEH−PPV, Vacar et al. concluded that the relaxed exciton state consisted of a single $\pi-\pi^*$ interband transition rather than a superposition of narrow absorptions from segments with different conjugation lengths.[16b] Alternatively, a molecular approach has been carried out by Rauscher et al.[42,43] that describes PPV as a random organic solid with an energy distribution of localized sites of different conjugation lengths. Since MEH−PPV and BEH−PPV differ only in their side chains, they can be considered very similar as far as π-conjugation is concerned. Because of strong interactions among monomer units and relatively high energies required for twisting these planar polymers into segmented nonplanar structures, the disorder in these polymers is likely a gradual deviation from a perfect planar conformation, analogous to twisting a stiff ribbon. In fact, only a 5−10° deviation from the planar conformation was observed in crystalline PPV.[34] Because of this gradual deviation from the planar conformation, the π-conjugation between adjacent units is largely undisturbed, resulting in the longest average conjugation length among the three polymers.

In the limit of strong π-conjugation, the initial exciton could move quickly along the chain to form relaxed emissive excitons or nonemissive species, such as free carriers or distant polarons, if the energies of the electrons and holes exceed their Coulombic interaction. If the π-conjugation length of the emissive exciton state is smaller than the shortest conjugation length in the polymer, the localized initial exciton state with a higher energy can quickly relax to the emissive exciton state with almost no barrier. Even when BEH−PPV is excited with photon energies well above the 0−0 transition, the relaxation time is too fast to resolve in our experiments, resulting in λ_{ex}-independent kinetics for the stimulated emission and photoinduced absorption (Tables 1 and 2, Figure 10).

For polymers **1** and **2**, the π-conjugation in their polymer chains is significantly attenuated because of the presence of nonplanar conformations. Even within a planar segment, bpy units create energy barriers for the electron delocalization due to weakened electronic interactions between two neighboring groups of different structures. Therefore, a polymer chain can be viewed as an ensemble of segments with different conjugation lengths[44] and the average π-conjugation length in polymers **2** is shorter than that in BEH−PPV and is even shorter in polymer **1**. When such a polymer is excited by photons of a particular energy, the initial excitons will be preferentially created within a group of segments of certain conjugation lengths. As in BEH−PPV, this initial exciton state will relax to the emissive exciton state. However, conjugation lengths in polymers **1** and **2** are likely shorter than the π-electron delocalization length of the emissive exciton state in BEH−PPV. Thus, the quantum confinement of the exciton occurs, producing two effects: (1) an increase of the potential barriers for forming nonemissive species (e.g., free electron carriers or distant polarons) and many-body processes (e.g., exciton−exciton annihilation), thus hindering nonradiative processes; (2) a decrease of the energy-transfer rate (or exciton diffusion rate) along the chain due to less electronic overlap and smaller, more segmented dipole moments. Overall, polymers **1** and **2** have segments that are more like molecular oligomers, whereas BEH−PPV is more like a one-dimensional semiconductor. The key difference is the electronic coupling between different segments of the polymer chain that regulates the dynamics of the exciton states.

When the polymers were excited by light with an energy well above the 0−0 transitions (e.g., 417 nm), the initial exciton state resides at segments with shorter conjugation lengths than the emissive exciton state. The observed spectral diffusion in the stimulated emission region reflects the energy-transfer process from the initial exciton to the emissive exciton state. This process takes less than 1 ps for BEH−PPV, about 50 ps for polymer **2**, and 100 ps for polymer **1.** When the polymers are excited by photons with a lower energy, the initial exciton will be preferentially created at those segments with a longer conjugation length. Because the energy difference between the initial exciton and the emissive exciton states is now smaller, the exciton diffusion path is shorter. When the emissive exciton state is excited directly, corresponding to excitation near the 0−0 transition, there is no exciton diffusion. Since spectral diffusion in BEH−PPV takes less than 1 ps even with the highest energy photons in our experiments, the lifetime of stimulated emission for BEH−PPV appears to be λ_{ex}-independent. The energy-transfer process is slowed considerably in polymer **2** because of the potential barriers for exciton diffusion. The stimulated emission of polymer **2** is clearly λ_{ex}-dependent [Figure 7b] with less deviation from the photoluminescence spectrum when λ_{ex} gets longer. When polymer **2** is excited by 536 nm light near its 0−0 transition, there is no spectral diffusion of its stimulated emission, which implies direct population of the emissive exciton state. The lifetime of the stimulated emission also decreases as λ_{ex} gets longer (Table 2), reflecting a decrease in diffusion from the initial exciton to the emissive exciton. More interestingly, the stimulated emission of polymer **2** has a component with a 14 ps rise time constant when it is excited by 417 nm light. Since the population of the emissive exciton state is determined by its intrinsic decay rate as well as its rate of formation, the origin of this rise component is likely due to continuous formation of the emissive exciton state through direct excitation or energy transfer from the initial exciton state. This rise component is more significant in polymer **1** (not shown) and has a longer time constant than polymer **2** because its π-conjugation is more fragmented and the initial exciton needs to cross more potential barriers in order to reach the relaxed emissive exciton state. Also, the coupling between

shorter dipoles with more diverse dipole orientations slows down the Förster energy-transfer process.

This three-state energy-transfer mechanism also agrees with the observed changes in the photoinduced absorption. The overall integrated intensity of photoinduced absorption increases with π-conjugation attenuation in polymer chains in the sequence of BEH−PPV, polymer **2**, and polymer **1**. Because the π-conjugation in these polymers is increasingly fragmented in the same order, the origins of the photoinduced absorption must have a localized nature. This conjecture can be confirmed by the λ_{ex} dependence of the overall integrated photoinduced absorption intensities. The high-energy photons, which excite initial excitons with shorter conjugation lengths, generate higher integrated photoinduced intensities (Figure 7). Moreover, the photoinduced absorption in PPV has been assigned to bound polaron pairs[15a] and the enhanced photoinduced absorption in MEH−PPV was used as evidence of carboxyl defects due to photooxidation that quenches the photoluminescence.[15b] Photooxidation should not be a significant source of photoinduced absorption in our study because the samples were kept under nitrogen and changed frequently during the laser experiments. The statement on the localized nature of the photoinduced absorption during the first nanosecond following the excitation does not contradict previous observations in the photooxidation in MEH−PPV[15] because the oxidized vinyl group also breaks the π-conjugation in MEH−PPV chains, causing π-electron localization. While previously observed photooxidation products quench the photoluminescence, the localized initial excitons in polymers **1** and **2** are converted to the relaxed emissive exciton state.

Finally, the three-state exciton dynamics model can also explain the enhanced photoluminescence yields of polymers **1** and **2** relative to that of BEH−PPV in terms of the formation of nonemissive species and the quantum confinement of excitons. Because of the well-conjugated structure and strongly interacting monomer units in BEH−PPV, the electrons and the holes in the initial excitons could diffuse rapidly, forming nonemissive free carriers and distant polarons if their energies are high enough to overcome the Coulombic interactions. When more than one exciton is created in the same polymer chain, exciton−exciton annihilation could occur because of the high mobility of the excitons. For polymers **1** and **2**, the probabilities of forming nonemissive species and exciton−exciton annihilation are smaller because of the reduced mobility for electrons and holes in the initial excitons due to the potential barriers generated by the bpy units. Because these nonradiative processes are greatly reduced, more initial excitons become available for conversion to the emissive exciton states, resulting in a higher photoluminescence quantum yield. The differences between BEH−PPV and polymer **2** in the branching ratio of radiative and nonradiative products can be seen by comparing the kinetics of photoinduced absorption, stimulated emission, and ground-state bleaching in Figure 11. The discrepancy among the three kinetics in BEH−PPV suggests that a significant fraction of the initial exciton becomes optically quiet and can be detected only via ground-state bleaching. The origin of the initial fast decay component in the ground-state bleaching is very likely due to nonradiative species decaying to the ground state via internal conversion. A similar observation was made in phenyl-substituted PPV (PPPV) where the photoluminescence lifetime and the quantum yield increase compared to those in PPV. These increases were attributed to more distorted π-conjugation in the polymer.[45]

Summary

Conjugated PPV type polymers in solution can be described as an ensemble of interacting oligomers. The electronic coupling between the oligomers determines the length of π-conjugation and the photophysics of the polymer. Attenuation of the coupling between the oligomers can be introduced by an electronic structural mismatch between adjacent monomers and by structural distortions from a planar conformation within an oligomeric segment. The bpy groups in polymers **1** and **2** accomplish both. Experimentally, we observed significant changes in the photophysics and dynamics in polymers **1** and **2** from those of BEH−PPV, which can be explained by a three-state exciton dynamics model that invokes an intramolecular energy transfer from higher energy localized initial excitons to lower energy relaxed emissive excitons. A polymer with strongly interacting oligomers facilitates high mobilities for the initial excitons, leading to effective formation of nonemissive species as well as fast exciton relaxation to the emissive exciton state. However, polymers with attenuated π-conjugation have more barriers for the excitons to move along the chain, which causes enhanced photoinduced absorption and higher photoluminescence quantum yields. On the basis of our study, a correlation between the π-conjugation and photophysics in conjugated polymer solutions is established at early times following photoexcitation. We have also investigated the effects of metal ion binding at the bpy groups on the photophysics of these polymers. These studies will be published separately.[46]

Acknowledgment. This work was supported by the Environmental Management Science Program and by the Division of Chemical Sciences, Office of Basic Energy Sciences, U.S. Department of Energy under Contract W-31-109-Eng-38. The authors thank Professors F. P. Spano and L. J. Rothberg for helpful discussions and comments.

References and Notes

(1) Burroughes, J. H.; Bradley, D. D.; Brown, A. R.; Marks, R. N.; Mackay, K.; Friend, R. H.; Burn, P. L.; Holmes, A. B. *Nature* **1990**, *347*, 539.

(2) For a recent review, see the following. Leising, G.; Tasch, S.; Graupner, W. In *Handbook of Conducting Polymers*; Skotheim, T. A., Elsenbaumer, R. L., Reynolde, J. R., Eds.; M. Dekker: New York, 1998; p 847.

(3) Friend, R. H.; Greenham, N. C. In *Handbook of Conducting Polymers*; Skotheim, T. A., Elsenbaumer, R. L., Reynolde, J. R., Eds.; M. Dekker: New York, 1998; p 823.

(4) Friend, R. H.; Denton, G. J.; Halls, J. J. M.; Harrison, N. T.; Holmes, A. B.; Köhler; Lux, A.; Moratti, S. C.; Picher, K.; Tessler, N.; Towns, K.; Wittmann, H. F. *Solid State Commun.ications* **1997**, *102*, 249.

(5) Tessler, N.; Denton, G. J.; Friend, R. H. *Nature* **1996**, *382*, 695.

(6) Hide, F.; Diaz-Garcia, M. A.; Schwartz, B. J.; Anderson, M. R.; Fei, Q.; Heeger, A. J. *Science* **1996**, *273*, 1833.

(7) Frolov, S. V.; Gellermann, W.; Ozak, M.; Yoshino, K.; Vardeny, Z. V. *Phys. Rev. Lett.* **1997** *78*, 729.

(8) Peng, Z.; Gharavi, A. R.; Yu, L. *J. Am. Chem. Soc.* **1997**, *119*, 4622.

(9) Wang, B.; Wasielewski, M. R. *J. Am. Chem. Soc.* **1997**, *119*, 12.

(10) Ley, K. D.; Whittle, E.; Bartberger, M. D.; Schanze, K. S. *J. Am. Chem. Soc.* **1997**, *119*, 3423.

(11) Kimura, M.; Horai, T.; Hanabusa, K.; Shirai, H. *Adv. Mater.* **1998**, *10*, 459.

(12) Davis, W. B.; Svec, W. A.; Ratner, M. A.; Wasielewski, M. R. *Nature*, in press.

(13) Jiang, H.; Yang, S.-W.; Jones, W. E., Jr. *Chem. Mater.* **1997**, *9*, 2031.

(14) In *Primary Photoexcitations in Conjugated Polymers: Molecular Exciton versus Semiconductor Band Model*; Sariciftci, N. S., Ed.; World Scientific: Singapore, 1998.

(15) (a) Yan, M.; Rothberg, L. J.; Papadimitrakopoulos, F.; Galvin, M. E.; Miller, T. M. *Phys. Rev. Lett.* **1994**, *72*, 1104. (b) Hsu, J. W. P.; Yan, M.; Jedju, T. M.; Rothberg, L. J. *Phys. Rev. B* **1994**, *49*, 712.

(16) (a) Schwartz, B. J.; Hide, F.; Andersson, M. R.; Heeger, A. J. *Chem. Phys. Lett.* **1997**, *265*, 327. (b) Vacar, D.; Dogariu, A.; Heeger, A. J. *Adv. Mater*. **1998**, *10*, 669.

(17) McBranch, D. W.; Sinclair, M. B. In *Primary Photoexcitations in Conjugated Polymers: Molecular Exciton versus Semiconductor Band Model*; Sariciftci, N. S., Ed.; World Scientific: Singapore, 1998; Chapter 20, p 587 and references therein.

(18) Leng, I. M.; Jeglinski, S.; Wei, X.; Bennerr, R. E.; Vardeny, Z. V.; Guo, F.; Mazumdar, S. *Phys. Rev. Lett.* **1994**, *72*, 156.

(19) Blatchford, J. W.; Jessen, S. W.; Lin, L. B.; Lih, J. J.; Gustafson, T. L.; Epstein, A. J.; Fu, D. K.; Marsella, M. J.; Swager, T. M.; MacDiamid, A. G.; Yamaguchi, S.; Hamaguchi, H. *Phys. Rev. Lett.* **1996**, *76*, 1513.

(20) Conwell, E. M.; Mizes, H. A. *Phys. Rev. B.* **1995**, *51*, 6953.

(21) Dyakonov, V.; Frankevich, E. *Chem. Phys.* **1998**, *227*, 203.

(22) Murata, K.; Shimoi, Y.; Abe, S.; Kuroda, S.; Noguchi, T.; Ohnishi, T. *Chem. Phys.* **1998**, *227*, 191.

(23) Shuai, Z.; Brédas, J. L.; Su, W. P. *Chem. Phys. Lett.* **1994**, *228*, 301.

(24) (a) Brédas, J. L.; Cornil, J.; Meyers, F.; Beljonne, D. In *Handbook of Conducting Polymers*; Skotheim, T. A., Elsenbaumer, R. L., Reynolde, J. R., Eds.; M. Dekker: New York, 1998; p 1. (b) Beljonne, D.; Cornil, J.; dos Santos, D. A.; Shuai, Z.; Brédas. In *Primary Photoexcitations in Conjugated Polymers: Molecular Exciton versus Semiconductor Band Model*; Sariciftci, N. S., Ed.; World Scientific: Singapore, 1998; Chapter 19, p 559.

(25) Janssen, R. A. J.; Sacriciftci, N. S.; Pakbas, K.; McNamara, J. J.; Schricker, S.; Heeger, A. J.; Wudl, F. *Synth. Met.* **1995**, *69*, 441.

(26) Hale, G. D.; Oldenburg, S. J.; Halas, N. J. *Phys. Rev. B.* **1997**, *55*, R16069.

(27) Smilowitz, L.; Heeger, A. J. *Synth. Met.* **1992,** *48*, 193.

(28) Kersting, R.; Mollay, B.; Rusch, M.; Wenisch, J.; Leising, G.; Kauffmann, H. F. *J. Chem. Phys*. **1997**, *106*, 2850.

(29) Hayes, G. R.; Samuel, I. D. W.; Phillips, R. T. *Phys. Rev. B* **1997**, *56*, 3838.

(30) Obrzut, J.; Karasz, F. E. *J. Chem. Phys.* **1987**, *87*, 2349.

(31) Denton, G. J.; Tessler, N.; Harrison, N. T.; Friend, R. H. *Phys. Rev. Lett*. **1997**, *78*, 733.

(32) Lee, C. H.; Yu, G.; Moses, D.; Heeger, A. J. *Synth. Met.* **1995**, *69*, 429.

(33) Hennecke, M.; Damerau, T. *Macromolecules* **1993**, *26*, 3411.

(34) Winokur, M. J. In *Handbook of Conducting Polymers*; Skotheim, T. A., Elsenbaumer, R. L., Reynolde, J. R., Eds.; M. Dekker: New York, 1998; p 707.

(35) Galasso, V.; De Alti, G.; Bigotto, A. *Tetrahedron* **1971**, *27*, 991.

(36) Greenfield, S. R.; Svec, W. A.; Gosztola, D.; Wasielewski, M. R. *J. Am. Chem. Soc*. **1996**, *118*, 6767.

(37) ZINDO/S is an INDO method parametrized to reproduce UV−visible spectroscopic transitions when used with the singly excited CI method. It was developed in the research group of Michael Zerner of the Quantum Theory Project at the University of Florida.

(38) Bässler, H.; Brandl, V.; Deussen, M.; Göbel, E. O.; Kersting, R.; Kurz, H.; Lemmer, U.; Mahrt, R. F.; Ochse, A. *Pure Appl. Chem.* **1995**, *67*, 377.

(39) Darsey, J. A.; Sumpter, B. G. *Prepr. Polym. Sci.* **1989**, *30*, 3.

(40) Fahlman, M.; Gebler, D. D.; Piskun, N.; Swager, T. M.; Epstein, A. J. *J. Chem. Phys.* **1998**, *109*, 2031.

(41) Graham, S. C.; Bradley, D. D. C.; Friend, R. H.; Spangler, C. *Synth. Met*. **1991**, *41*, 1277.

(42) Rauscher, U.; Schütz, L.; Greiner, A.; Bässler, H. J. *J. Phys.: Condens. Matter* **1989**, *1*, 9751.

(43) Rauscher, U.; Bässler, H. J.; Bradley, D. D. C.; Hennecke, M. *Phys. Rev. B* **1990**, *42*, 9830.

(44) Bässler, H. In *Primary Photoexcitations in Conjugated Polymers: Molecular Exciton versus Semiconductor Band Model*; Sariciftci, N. S., Ed.; World Scientific: Singapore, 1998; Chapter 3, p 51 and references therein.

(45) Lemmer, U.; Göbel, E. O. In *Primary Photoexcitations in Conjugated Polymers: Molecular Exciton versus Semiconductor Band Model*; Sariciftci, N. S., Ed.; World Scientific: Singapore, 1998; Chapter 9, p 211.

(46) Chen, L. X.; Jäger, W. J. H.; Niemczyk, M. P.; Wasielewski, M. R. To be published.